Nat. Hazards Earth Syst. Sci. Discuss., 3, 7555–7586, 2015
www.nat-hazards-earth-syst-sci-discuss.net/3/7555/2015/
doi:10.5194/nhessd-3-7555-2015


Natural Hazards and Earth System Sciences
Open Access
Discussions



# An extended stochastic method for seismic hazard estimation

**A. K. Abd el-aal[1], M. A. El-Eraki[2], and S. I. Mostafa[2]**

[1]National Research Institute of Astronomy and Geophysics (NRIAG), Helwan, Egypt
[2]Geology Department, Faculty of Science, Zagazig University, Zagazig, Egypt

Received: 14 October 2015 – Accepted: 29 November 2015 – Published: 21 December 2015

Correspondence to: S. I. Mostafa (high_dam83@yahoo.com)

Published by Copernicus Publications on behalf of the European Geosciences Union.

## Abstract

In this contribution, we developed an extended stochastic technique for seismic hazard assessment purposes. This technique depends on the hypothesis of stochastic technique of Boore (2003) "Simulation of ground motion using the stochastic method. Appl. Geophy. 160:635–676". The essential characteristics of extended stochastic technique are to obtain and simulate ground motion in order to minimize future earthquake consequences. The first step of this technique is defining the seismic sources which mostly affect the study area. Then, the maximum expected magnitude is defined for each of these seismic sources. It is followed by estimating the ground motion using an empirical attenuation relationship. Finally, the site amplification is implemented in calculating the peak ground acceleration (PGA) at each site of interest. We tested and applied this developed technique at Cairo, Suez, Port Said, Ismailia, Zagazig and Damietta cities to predict the ground motion. Also, it is applied at Cairo, Zagazig and Damietta cities to estimate the maximum peak ground acceleration at actual soil conditions. In addition, 0.5, 1, 5, 10 and 20 % damping median response spectra are estimated using the extended stochastic simulation technique. The calculated highest acceleration values at bedrock conditions are found at Suez city with a value of 44 cm $s^{-2}$. However, these acceleration values decrease towards the north of the study area to reach 14.1 cm $s^{-2}$ at Damietta city. This comes in agreement with the results of previous studies of seismic hazards in northern Egypt and is found to be comparable. This work can be used for seismic risk mitigation and earthquake engineering purposes.

## 1 Introduction

Seismic hazard is defined as the probable level of ground shaking associated with the recurrence of earthquakes. It is applied in reducing economic and social effects of earthquake disasters through the prediction of ground motion and related damage scenarios. Seismic hazard can be assessed using probabilistic seismic hazard approach

(PSHA) and/or deterministic seismic hazard approach (DSHA). PSHA is considered as seismology's most valuable contribution to earthquake hazard assessment (Reiter, 1990; Frankel, 1995; Woo, 1996; Giardini, 1999; Bommer et al., 2004; Deif et al., 2009; El-Hussain et al., 2010; Rafi et al., 2013; Ur-Rehman et al., 2013a, b). It uses all the available historical and instrumental earthquake data to estimate the seismic hazard. Nevertheless, when a complete earthquake catalogue is unavailable for a study area, DSHA can be utilized to estimate the seismic hazard. DSHA amounts to identify and select the worst case earthquake (McGuire, 2001; Anderson et al., 2000; Anderson, 1997) which will produce the most severe ground motion at the investigated site. Both of these analyses require previous knowledge about seismicity, tectonics, geology and attenuation characteristics of seismic waves.

Another technique that can be used in assessing the seismic hazard in an area is the stochastic simulation method. This technique combines parametric or functional descriptions of the ground motion's amplitude spectrum with a random phase spectrum modified such that the motion is distributed over a duration related to the earthquake magnitude and to the distance from the source. It is based on the point source assumption and it is well known that this assumption fails in the near source region of large earthquakes. It is useful for simulating the high frequency ground motions of most interest to engineers ($f > 1$ Hz). This method defines the ground motion at the study site in terms of peak ground acceleration (PGA), peak ground displacement (PGD) and peak ground velocity (PGV). One of the essential characteristics of this method is that the total spectrum of the motion at a site is formed of contributions from earthquake source, path and site. By separating the spectrum into these components, the stochastic models can be easily modified to account for specific situations or to account for improved information about particular aspects of the model (Boore, 2003). Thus, assessing the ground motion at any site located at a given distance from an earthquake of given magnitude is one of the most critical elements of any seismic hazard analysis (Abd El-Aal, 2008, 2010a).





NHESSD
3, 7555–7586, 2015

Earthquakes are considered as the most typical phenomena of natural hazard. They influence human life, bridges, railway, buildings, strategic projects and man-made structures. Frequent large earthquakes in remote areas determine high seismic hazard but pose no risk. However, moderate earthquakes in densely populated areas imply small hazard with high risk. In Egypt, buildings are not designed to resist earthquakes. Therefore, relatively small events can be the source of huge socio-economic disasters. The north eastern part of Egypt was affected by many earthquakes like 31 March 1969 ($M_w = 6.9$), 29 April 1974 (Abu-Hammad earthquake with $M_w = 5.11$), 12 June 1983 ($M_w = 5.28$), 29 March 1984 ($M_w = 5.11$), 2 January 1987 (Ismailiya earthquake with $M_w = 5.28$), 12 October 1992 ($M_w = 5.8$), 22 November 1995 ($M_w = 7.3$), 28 December 1999 ($M_w = 4.5$) and 24 August 2002 ($M_w = 4.3$) earthquakes. In cities with vibrant economy, large earthquake may cause an economic downturn lasting for a long period of time. This can be avoided by the development of better construction methods, safety systems, early warning and effective evacuation planning.

Previous studies were applied in different parts of the study area to assess seismic hazard (El-Eraki et al., 2015; Abd El-Aal, 2010a, b; El-Sayed et al., 2001; Sadek, 2010). In the current study, seismic hazard is assessed using a new extended stochastic simulation method. This method is developed basing on the stochastic technique of Boore (2003) for the purpose of earthquake resistant structures or seismic safety assessment. The developed extended stochastic simulation method is applied to predict the ground motion at Cairo, Suez, Port Said, Ismailia, Zagazig and Damietta cities (Fig. 2) which are of high socio-economic importance in Egypt. It is used in terms of peak ground acceleration and response spectra to acquire a quantitative evaluation of the nature of ground shaking from future earthquakes.

## 2 Method

In this paper, a new extended stochastic simulation technique is developed based on the hypothesis of the stochastic method of Boore (2003) to predict the seismic hazard.





NHESSD
3, 7555–7586, 2015

Figure 1 illustrates components and steps of the new developed extended stochastic technique. The total spectrum of the ground motion in this developed method is consists of earthquake sources, path, site and instrument. These terms can be involved in a general equation (Boore, 2003), in the frequency domain, as follow:

$$Y(M_0,R,f) = E(M_0,f)\,P(R,f)\,G(f)\,I(f) \quad (1)$$

where $Y(M_0,R,f)$ is the Fourier amplitude spectrum of ground acceleration (gathering the seismic moment and the distance), $E(M_0,f)$ is the earthquake source spectrum for a specific seismic moment, $P(R,f)$ is the path which models the geometric spreading and the anelastic attenuation effects as a function of $R$ and $f$ (the hypocentral distance and frequency, respectively), $G(f)$ is the site effect and $I(f)$ is the instrumental transfer function and it represents a filter that characterizes the spectrum to get some particular type of the ground motion (displacement, velocity or acceleration).

## 2.1 Source parameters

The input source parameters required for the developed extended stochastic simulation at an area are described in the following:

### 2.1.1 Definition of seismic sources

The definition of seismic sources depends on the interpretation of geological, geophysical and seismological data. The seismotectonic source model is defined as the geographical distribution of seismic source zones and the specification of all source parameters required for seismic hazard assessment (Abd el-aal et al., 2015; El-Hussain et al., 2010). In general, a source zone can be idealized as a point source, a line source, an area source, a volume source or a dipping plane (Lee and Trifunace, 1985).

The seismotectonic source model is prepared depending on the spatial distribution of large, moderate and small earthquakes having close characteristics like the focal mechanism to finally obtain a seismic zone that have the same possibility of future





NHESSD
3, 7555–7586, 2015

earthquakes to be occurred in any point inside it. It is preferable to convert all events in the catalogue that is used in constructing the seismic model to the moment magnitudes ($M_w$) scale as it is the most reliable magnitude scale. Any duplication in the catalogue events should be removed. Catalogue declustering should also be done by removing the dependent events (foreshocks and aftershocks) to satisfy the spatial and temporal principles of earthquakes independency.

The source parameters in the stochastic model involve some parameters (Boore, 2003) like the average radiation pattern for the shear waves which has a value of about 0.55, the free surface amplification, the reduction factor that represents the partitioning of energy into two horizontal components (usually taken as $1/\sqrt{2}$), the density and the shear wave velocity.

#### 2.1.2 Definition of maximum expected magnitude

It is essential to define the maximum expected magnitude for each of the identified seismic sources. This is because it has a considerable influence on the seismic hazard, especially at long return periods and short distances from the sites of interest. The maximum expected magnitude can be estimated by four different procedures: (1) using the results of paleoseismological studies, if present, (2) using the statistical procedure proposed by Kijko (2004), if the seismic history is available, (3) using the fault rupture, if reliable data concerning fault type and its total length are available, the maximum expected magnitude can be estimated by assuming that 20 to 40 % from the total fault length could rupture in one earthquake and (4) using a constant increment (0.5 magnitude unit) to largest known magnitude in each seismogenic zone.

### 2.2 Path parameters

The effect of travel path from source to site on the ground motion depends on geometrical spreading and attenuation (both intrinsic attenuation and scattering attenuation)





NHESSD
3, 7555–7586, 2015

that influence the spectrum of motion at a particular site. The simplified path effect $P$ is obtained using the following formula (Boore, 2003, 2009):

$$P(R,f) = Z(R)\exp\left[-\frac{\pi f R}{Q(f)C_Q}\right] \quad (2)$$

where $Z(R)$ is the geometrical spreading function, $Q$ is the anelastic attenuation function, $C_Q$ is the seismic velocity used in the determination of $Q(f)$ and $R$ is the closest distance to the rupture surface.

### 2.3 Site parameters

Generally, the modification of seismic waves by local site conditions is part of the path effect. This is because local site effects are largely independent of distance traveled from the source, except for nonlinear effects for which the amplitudes of motion are important. Sites having soft sediments tend to increase the ground motion in comparison to bedrock sites. This is because at sites with exposed soft soil or having topographic undulation, the seismic energy is trapped due to the impedance contrast between sediments and the underlying bedrock. This leads to a resonance patterns and thus amplifies the ground motion (Lacave et al., 1999). The site effect $G(f)$ is a combination of the amplification $A(f)$ and the attenuation $D(f)$ (Boore, 2003) as follows:

$$G(f) = A(f) + D(f). \quad (3)$$

The amplification vectors $A(f)$ is relative to the source unless amplitude variations due to wave propagation, separate from the geometrical spreading, have been accounted for. The diminution or attenuation function $D(f)$ is used to model the path independent loss of energy. This loss of energy may be due to a source effect (Papageorgiou and Aki, 1983), a site effect (Hanks, 1982) or by a combination of these effects. If source effect, the attenuation may also depend on the size of the earthquake. In order to account for the high cut filter, the following equation (Boore, 1983) is used:





NHESSD
3, 7555–7586, 2015

$$D(f) = \left[1 + \left(\frac{f}{f_{max}}\right)^8\right]^{-1/2} \quad (4)$$

where $f_{max}$ is the high frequency cutoff. It is equal to 20 Hz or it is equal to 15 Hz for soft surface layers and 25 Hz for bedrock (Hanks, 1982).

### 2.4 Ground motion simulation

Once the maximum earthquake magnitude is defined for each seismic source, the corresponding ground motion at the investigated sites of interest should be estimated. Given the spectrum of motion at a site, the ground motion can be obtained through two ways: (1) time domain (TD) simulation and (2) random vibration (RV) theory. The time domain simulation can be useful in estimating the peak parameters such as the peak acceleration, peak velocity and peak displacement. A much quicker way in estimating the peak parameters is through using the random vibration theory, but it is not useful if time series are required in the analysis. Also, there are assumptions in the random-vibration theory that are not present in the time domain simulation. For this reason, time domain simulation is used in this study as it can be considered as truth. In general, the ground motion calculation is made by assuming that the maximum earthquakes are located at the closest distances to the sites of interest.

### 2.5 Seismic hazard estimation

The developed extended stochastic simulation technique is used to estimate the seismic hazard in terms of PGA, PGV and PGD. First, the seismic source of a possible impact on the site of interest is defined. Then, an earthquake of maximum magnitude is assigned to each of the seismic sources. It is followed by determining the closest distance of each source from the site of interest. Then, the ground motion is calculated using appropriate attenuation relationships. Finally, the site parameters are used in





NHESSD
3, 7555–7586, 2015

calculating the PGA at different periods for each site. The seismic source that has the strongest ground motion (represented in the highest values of PGA, PGV and PGD) at a site of interest, represents the source of the most hazardous effect at this site.

## 3 Case study

The new extended stochastic simulation method is used here to assess the seismic hazard at Cairo, Suez, Port Said, Ismailia, Zagazig and Damietta cities (Fig. 2) which are located in the north-eastern part of Egypt. The study area is located between latitudes 29°54′32.4″ and 31°39′18″ N and longitudes 31°0′36″ and 32°59′9.6″ E.

### 3.1 Geological, structural and seismological settings

The study area includes the eastern part of the Nile Delta and the north-western part of Sinai. Its surface is mostly covered by Quaternary deposits and consists of sand dunes, sabkha deposits and undivided Quaternary deposits consisting of wadi deposits, playa deposits and raised beaches. Quaternary Nile deposits and Pliocene deposits consisting of marine beds are exposed on the surface of the eastern Nile Delta. The surface of the area of study is also covered by Miocene deposits that are represented by clastics, gypsum and carbonates. Basalt dolerite dykes and sheets mainly of Tertiary age are exposed in some localities. The Oligocene deposits consist of fluviatiles, lacustrine clastics and gravel sheets between Cairo and Suez and around Cairo. Surface Eocene deposits consist of thick marine limestone with chert and minor clay beds. Undivided Cretaceous rocks are exposed in some localities. In northern Sinai, the Upper Cretaceous deposits consist mainly of carbonate beds and the Jurassic rocks are represented by marine and associated fluviomarine beds (Geologic Map of Egypt, 1981).

The structural setting of the study area is characterized by a complicated pattern formed of faults and folds. Faults in eastern Nile Delta are of normal type and strike mainly in the E-W and NW–SE directions. Folds have a relatively minor importance





NHESSD
3, 7555–7586, 2015

and observed at few localities on the surface such as Gebel Subrawit and Gebel Iwabid (El-Fayoumy, 1968). In subsurface, these major folds were truncated by faults and consequently allowed the high pressure water bearing Nubia Sandstone strata to be uplifted close to the surface (El-Dairy, 1980). However, northern Sinai is characterized by the presence of NE to ENE oriented doubly plunging anticlines. These anticlines include large, intermediate and small folds. Six E-NE elongated belts of right-stepped en-echhelon folds are recognized. These fold belts probably overlie deep seated faults rejuvenated by right lateral transpression in late Cretaceous-early Tertiary time (Said, 1990).

Egypt is one of the few regions of the world where evidences of historical earthquake activity have been documented during the past 4800 years. Many events were reported to have occurred in and around Egypt and affected the study area such as 2200 BC (Tell Basta earthquake), 4 October AD 935 earthquake, 26 May 1111 East Cairo earthquake, 8 August 1303 (Eastern Mediterranean earthquake), 5 March AD 1455 earthquake, September AD 1754 earthquake, 7 December AD 1895 earthquake (Sieberg, 1932; Ambraseys, 1961; Maamoun, 1979; Ibrahim and Marzouk, 1979; Poirier and Taher, 1980; Savage, unpublished data; Kebeasy, 1990; Ambraseys et al., 1994). The study area is affected also by instrumental earthquakes that have been recorded in Egypt since 1899. These earthquakes are ranging from micro, small, medium to strong earthquakes. Consequently, the study area is characterized by a moderate seismic activity.

Seismicity in Egypt tends to occur along the active margins of the plate boundaries: African plate, Eurasian plate, Arabian plate and Sinai sub-plate. Almost all the seismic activity of Egypt is concentrated in the northern part of its territory. It is affected by regional and local active seismic sources. Regionally, the seismotectonics in Egypt is related to the regional tectonics of the Mediterranean Sea and the Red Sea (Maamoun and Ibrahim, 1978; Maamoun et al., 1980; Kebeasy et al., 1981; Ibrahim, 1985; Albert, 1987; Kebeasy, 1990; Degg, 1990; Abou Elenean, 1993). The local seismic activity is located at specific seismic zones that reflect their tectonic activities. These zones





NHESSD
3, 7555–7586, 2015

have different levels of seismic activity like south east Mediterranean Sea zone, central Negev shear zone, central Sinai fault zone, northern Red Sea, Dahshour (south-west Cairo), Abu Zabal, Gulf of Suez, Gulf of Aqaba and Cairo-Suez district zones.

### 3.2 Application of the newly developed stochastic method

The developed extended stochastic method is applied here to simulate the ground motion at Cairo, Suez, Port Said, Ismailia, Zagazig and Damietta cities. The seismic source model (Fig. 3) used in this study is updated from the seismotectonic model prepared by El-Eraki et al. (2015). The updated model used here is an area source model where every point has the same probability of being the epicenter of a future earthquake. This model is prepared depending on the spatial distribution of large, moderate and small instrumental earthquakes. It includes instrumental earthquake data having magnitudes ≥ 3 from the period of 1900 to 2011. The total number of dependent earthquakes in this model is 10 640 events.

This model contains thirty eight seismic sources as well as a background seismic zone which models the floating earthquakes that are located outside these distinctly defined zones. The most effective seismic source on each site is determined depending on the closest distance and the highest magnitude affecting the site. The maximum expected earthquake magnitude (Table 1) for each seismic zone is calculated using the statistical procedure proposed by Kijko (2004). The ground motion is simulated from four effective seismic sources (Table 2) which have the most considerable seismic effect on the sites under study. The closest epicentral distances between Suez, Cairo, Ismailia, Zagazig, Port Said and Damietta cities and the corresponding effective seismic sources are found to be 13.4, 13.9, 16.5, 26.4, 25.5 and 40.7 km, respectively. The density and the shear wave velocity, which are utilized in estimating the source parameters in the stochastic model, are taken for the average crustal properties in the study area and equal to 2.8 $\mathrm{gm\,cm^{-3}}$ and 3.8 $\mathrm{km\,s^{-1}}$, respectively.

The geometrical spreading relationship of Atkinson and Boore (1995) and the attenuation model of Moustafa (2002) are applied here to account for the effect of travel path from the seismic source to the investigated site on the ground motion. In order to account for the high cut filter, a high frequency cutoff value of 20 Hz is used because of the absence of strong motion records in Egypt suitable for its empirical determination. Also, this value preserves the interested frequencies (up to 10 Hz) for the engineering purposes.

The ground motion is simulated using the computer code SMSIM (Boore, 2009). It is simulated at Cairo, Zagazig and Damietta cities on surface soil because of the validity of the amplification data at these cities. However, there were no available amplification data at Suez, Portsaid and Ismailia cities. So, the stochastic simulation at these cities is done only on bedrock where the amplification and the corresponding fundamental resonance frequency are assumed to be 1 and 1 Hz, respectively.

The predicted ground motion for bedrock shows the highest acceleration at Suez city. It is followed by Cairo, Ismailia, Zagazig, Port Said and Damietta cities (Figs. 4 and 5). Also, the predicted ground motion for surface soil shows that the highest acceleration is at Cairo city. It is followed by Zagazig and Damietta cities (Fig. 6). These results (Table 2) show that the highest values are concentrated at the south-eastern part of the study area and decrease towards the north direction.

Response spectra are defined on the basis of the response of a single degree of freedom damped oscillator to the earthquake acceleration (Jennings, 1983). It serves two-fold function characterizing the ground motion as a function of frequency. The response spectra (0.5, 1, 5, 10 and 20 % damped pseudo-acceleration) for frequencies ranging from 0 to 25 Hz were simulated for the four effective seismic sources (Figs. 7 and 8). The results of pseudo-spectral acceleration (PSA) show that the highest PSA value is at Cairo city. It is followed by Suez, Ismailia, Zagazig, Port Said and Damietta cities. These results could be used as a base for design motion specification of the critical structure and for the nonlinear analysis (structural, site response, landslides and liquefaction).



Discussion Paper | Discussion Paper | Discussion Paper | Discussion Paper |

NHESSD

3, 7555–7586, 2015

An extended stochastic method for seismic hazard estimation

A. K. Abd el-aal et al.

Title Page
Abstract Introduction
Conclusions References
Tables Figures
◂ ▸
Back Close
Full Screen / Esc
Printer-friendly Version
Interactive Discussion

## 4 Comparison between the developed extended stochastic method and the probabilistic seismic hazard approach

The extended stochastic simulation method is applied at Cairo, Zagazig and Damietta cities to estimate the peak ground accelerations on surface soil at different frequencies. Information about site amplifications (Table 3) in the uppermost 30 m layer at these cities is taken from previous studies (Toni, 2007; Abdel-Rahman et al., 2010; Moustafa, 2013). These studies used the microtremor survey to obtain the peak amplification and its corresponding fundamental resonance frequency at each site. The results are plotted (Fig. 9) with the PGA on the vertical axis and the period (reciprocal of frequency) on the horizontal axis. In this figure, Fig. 9a shows the highest PGA value at Zagazig city and the lowest PGA value at Damietta city. However, Fig. 9b and c show the highest PGA value at Cairo city and the lowest PGA value at Damietta city to the north of the study area. This reveals the effect of the site amplification on the PGA values as it gives the highest PGA value at the sites that expose the highest amplification.

These results are comparable with the results (Table 4) of the work made by El-Eraki et al. (2015) who studied seismic hazard on our study area using the probabilistic seismic hazard approach (PSHA) (Fig. 10). They calculated the uniform hazard spectra (UHS) on bedrock for 75 and 475 years return periods. These return periods correspond to 80 and 90 % probability of non-exceeding ground motion in 50 years period (that is the expected design life for a building). Their results demonstrate that Cairo city exposes the most hazardous effect. This hazard diminishes toward the north direction of the study area at Damietta city.

## 5 Discussion and conclusions

In this work, a new extended stochastic simulation technique is developed basing on the stochastic method of Boore (2003) to assess the seismic hazard. This method is simple and powerful in simulating the ground motion in terms of PGA, PGD and

PGV. The ground motion is largely affected by the earthquake magnitude that can be assigned to the seismotectonic source that is mostly affecting the study site and on the source to site distance in a direct relationship.

The extended stochastic method is applied here to simulate the expected ground motion at some sites in the north-eastern part of Egypt. This region is important due to its location in the north-eastern part of Africa. It is affected by the movement of the African plate, Eurasian plate, Arabian plate and Sinai sub-plate. This movement controls the seismicity of the area at the regional scale. The results of the simulation give the highest hazardous effect at the south-eastern and the southern parts of the study area. The hazard is diminishes at Port Said and Damietta cities to the north direction of the study area.

The simulated PGA, PGD and PGV give the highest values on soft soil rather than bedrock reflecting the effect of local site conditions on seismic hazard. This is because of the impedance contrast between soil and bedrock which causes the multiple reflections of seismic waves in the layers near the ground surface. This leads to long duration of vibration and thus increases the hazardous effect on man-made structures. Also, the 0.5, 1, 5, 10 and 20 % damped pseudo-acceleration gives high values of PSA in the southern part of the study area. These values decrease to the north and to the west of the area of study.

In addition, the maximum peak ground accelerations at different frequencies (especially, the frequencies of main interest to the earthquake engineers) are estimated to identify its relation with the amplification. So, the PGAs are estimated at frequencies ranging from 0.4 to 10 Hz (corresponding to period ranging between 0.1 and 2.5 s) at Cairo, Zagazig and Damietta cities. It gave the highest PGA at the highest amplification indicating that the highest level of ground motion will be at the fundamental resonance frequency of the site. This means that the site of high ground motion amplification exposes high peak ground motion acceleration value. These results reinforce the fact of exceeding the ground motion on soft soil rather than hard rock. This work can be useful in earthquake engineering purposes before the construction of any structure to mitigate the hazardous effect at the study sites.

*Acknowledgements.* The authors thank the Egyptian National Seismic Network for providing earthquake catalogs and software.

## References

Abd el-aal, A. K.: Simulating time-histories and pseudo-spectral accelerations from the 1992 Cairo Earthquake at the proposed El-Fayoum New City Site, Egypt, Acta Geophys., 56, 1025–1042, doi:10.2478/s11600-008-0054-6, 2008.

Abd el-aal, A. K.: Modelling of seismic hazard at the northeastern part of greater Cairo metropolitan area, Egypt, J. Geophys. Eng., 7, 75–90, doi:10.1088/1742-2132/7/1/007, 2010a.

Abd El-Aziz Khairy Abd El-Aal: Ground motion prediction from nearest seismogenic zones in and around Greater Cairo Area, Egypt, Nat. Hazards Earth Syst. Sci., 10, 1495–1511, doi:10.5194/nhess-10-1495-2010, 2010b.

Abd el-aal, A. K., Kamal, H., Abdelhay, M., and Elzahaby, K.: Probabilistic and stochastic seismic hazard assessment for wind turbine tower sites in Zafarana Wind Farm, Gulf of Suez, Egypt, Bull. Eng. Geol. Environ., doi:10.1007/s10064-015-0717-x, in press, 2015.

Abd El-Rahman, K., Abd El-Aal, A. K., El-Hady, S. M., Mohamed, A. A., and Abdel-Moniem, E.: Fundamental site frequency estimation at new Domiat city, Egypt, 2010, Arab. J. Geosci., 5, 653–661, doi:10.1007/s12517-010-0222-2, 2010.

Abou Elenean, K. M.: Seismotectonics of the Mediterranean region, North of Egypt and Libya, MSc Thesis, Fac. Sci. Mansoura Univ. Egypt, 1993.

Albert, R. N. H.: Earthquake activity in Cairo-Suez district compared with the fault pattern from satellite photographs considering Egyptian large scale construction plan, Bull. Int. Inst. Seismol. Earthq. Eng., 22, 27–40, 1987.

Ambraseys, N. N.: On the seismicity of southwest Asia (data from XV century Arabic manuscript), Revue Pour L'etude des calamites, Geneve, 34, 18–30, 1961.

Ambraseys, N. N., Melville, C. P., and Adams, R. D.: The Seismicity of Egypt, Arabia, and the Red Sea, Cambridge Univ. Press., 181 pp., 1994.

Anderson, J. G.: Benefits of scenario ground motion maps, Eng. Geol., 48, 43–57, 1997.

Anderson, J. G., Brune, J. N., Anooshehpoor, R., and Ni, S.: New Ground motion data and concepts in seismic hazard analysis, Curr. Sci., 79, 1278–1290, 2000.
Atkinson, G. M. and Boore, D. M.: Ground motion relations for eastern North America, B. Seismol. Soc. Am., 85, 17–30, 1995.
Bommer, J. J., Abrahamson, N. A., Strasser, F. O., Pecker, A., Bard, P.-Y. H., Cotton, F., Fäh, D., Sabetta, F., Scherbaum, F., and Studer, J.: The challenge of defining upper bounds on earthquake ground motions, Seismol. Res. Lett., 75, 82–95, 2004.
Boore, D. M.: Stochastic simulation of high frequency ground motions based on seismological models of the radiated spectra, B. Seismol. Soc. Am., 73, 94–1865, 1983.
Boore, D. M.: Simulation of ground motion using the stochastic method, Pure Appl. Geophys., 160, 635–676, 2003.
Boore, D. M.: SMSIM-Fortran programs for simulating ground motions from earthquakes, Version 2.3, A Revision of OFR 96-80-A, US Geological Survey Open-File Report, US Geological Survey, USA, 2009.
Degg, M.: Egypt, in: Earthquake Hazards Atlas, Based on the R. O. A. Earthquake azard Zonation Scheme, edited by: Doornlamp, J. C., Reinsurance Offices Association, London, UK, 1990.
Deif, A., Elenean, K. A., El Hadidy, M., Tealeb, A., and Mohamed, A.: Probabilistic seismic hazard maps for Sinai Peninsula, Egypt, J. Geophys. Eng., 6, 288–297, 2009.
El-Dairy, M. D.: Hydrogeological studies on the eastern part of the Nile Delta using isotopes techniques, MSc Thesis, Fac. Sci. El-Azhar Univ. Egypt, 220, 1980.
El-Eraki, M. A., Abd el-aal, A. K., and Mostafa, S. I.: Multi-Seismotectonic Models, Present-Day Seismicity and Seismic Hazard Assessment for Suez Canal and its Surrounding Area, Egypt, Bull. Eng. Geol. Environ., Springer Verlag, Berlin, Heidelberg, doi:10.1007/s10064-015-0774-1, 2015.
El-Fayoumy, I. F.: Geology of groundwater supplies in the eastern region of the Nile Delta, PhD Thesis, Fac. Sci. Cairo Univ., Cairo, 207 pp., 1968.
El-Hussain, I., Deif, A., Al-Jabry, K., Al-Hashmi, S., Al-Toubi, K., Al-Shijby, Y., and Al-Saify, M.: Probabilistic and deterministic seismic hazard assessment for Sultanate of Oman, (Phase I) Project #22409017, Sultan Qaboos Univ Oman, submitted, 202 pp., 2010.
El-Sayed, A., Vaccari, F., and Panza, G. F.: Deterministic seismic hazard in Egypt, Geophys. J. Int., 144, 555–567, 2001.





NHESSD
3, 7555–7586, 2015

Frankel, A.: Mapping seismic hazard in the Central and Eastern United States, B. Seismol. Soc. Am., 66, 8–2, 1995.
Geologic Map of Egypt, Map Scale 1 : 2 000 000, Egyptian Geol. Sur. Min., Abbassiya, Cairo, Egypt, 1981.
Giardini, D.: The Global Seismic Hazard Assessment Program (GSHAP), Inst. Geophys. ETHZ Zurich, Zurich, Switzerland, 1992/1999, 957–974, 1999.
Hanks, T. C.: $F_{max}$, B. Seismol. Soc. Am., 72, 79–1867, 1982.
Ibrahim, E. M.: Seismic activity in the different tectonic provinces of Egypt, Bull. Int. Inst. Seismol. Earthq. Eng., 21, 139–176, 1985.
Ibrahim, E. M. and Marzouk, I.: Seismotectonic study of Egypt, Bull Helwan Inst. Astronom. Geophys., 191 pp., 1979.
Jennings, P. C.: Engineering seismology Proc Int School Physics 'Enrico Fermi', Course LXXXV, edited by: Kanamori, H. and Boschi, E., 138–173, 1983.
Kebeasy, R. M.: Seismicity, in: The Geology of Egypt, edited by: Said, R., Balkema, Rotterdam, 51–59, 1990.
Kebeasy, R. M., Maamoun, M., Albert, R. N. H., and Megahed, M.: Earthquakes activity and earthquakes risk around Alexandria, Egypt, Bull. Int. Inst. Seismol. Eng. Earthq. (IISEE), 19, 93–113, 1981.
Kijko, A.: Estimation of the maximum earthquake magnitude, $M_{max}$, Pure Appl. Geophys., 161, 81–1655, 2004.
Lacave, C., Bard, P.-Y., and Koller, M. G.: Microzonation: Techniques and Examples, in: Block 15: Nat Erdbebenrisiko (electronic book on the Internet; www.ndk.ethz.ch/pages/publ/Koller.pdf, last access: December 2015), 1–23, 1990.
Lee, V. W. and Trifunac, M. D.: Uniform Risk Spectra of Strong Earthquake Ground Motion, Dept. Civil Engineer. Univ. Southern California, Los Angeles, California, 5–80, 1985.
Maamoun, M.: Macroseismic observation of principal earthquakes in Egypt, Bull. Helwan Inst. Astronom. Geophys., 183, 1979.
Maamoun, M. and Ibrahim, E.: Tectonic activity in Egypt as indicated by earthquakes, Bull Helwan Inst Astronom Geophys Helwan Egypt, 170, 1–13, 1978.
Maamoun, M., Allam, A., Megahed, A., and Abu El-Ata, A.: Neotectonics and seismic regionalization of Egypt, Bull. Inter. Ins. Seismol. Earthq. Eng. (BIISEE), 18, 27–39, 1980.
McGuire, R. K.: Deterministic vs. probabilistic earthquake hazards and risks, Soil Dyn. Earthq. Eng., 21, 377–384, 2001.





NHESSD
3, 7555–7586, 2015

Moustafa, S.: Assessment of ground motion variation for seismic hazard mitigation in the vicinity of Cairo metropolitan area, PhD Thesis, Ain Shams Univ. Cairo, Cairo, Egypt, 2002.
Moustafa, S. I.: Engineering Seismological Studies for Sharkia Governorate, East Nile Delta, Egypt, MSc, Fac. Sci. Zagazig Univ., 209 pp., 2013.
Papageorgiou, A. S. and Aki, K.: A specific barrier model for the quantitative description of inhomogeneous faulting and the prediction of strong ground motion, Part II. Applications of the model, B. Seismol. Soc. Am., 73, 953–978, 1983.
Poirier, I. P. and Taher, M. A.: Historical seismicity in the near and middle east, north Africa and Spain from Arabic documents (VIIIth–XVIIth century), B. Seismol. Soc. Am., 70, 2185–2201, 1980.
Rafi, Z., Ahmed, N., Ur-Rehman, S., Azeem, T., and Abd el-aal, A. K.: Analysis of Quetta-Ziarat earthquake of 29 October, 2008 in Pakistan, Arab. J. Geosci., 6, 1731–1737, 2013.
Reiter, L.: Earthquake Hazard Analysis, Columbia University Press, New York, 254 pp. 1990.
Sadek, W.: Ground motion simulation of the Dahshour dislocation zone, BSc, Fac. Sci. Alex. Univ. Egypt, 161, 2010.
Said, R.: The Geology of Egypt, A. A. Balkema, Rotterdam, 431–486, 1990.
Sieberg, A.: Untersuchungen ueber Erdbeben und Bruchschollenbau im Oestlichen Mittelrmeergebiet, Denkschriften der Med. Nat. Ges. zu Jena, 18, 2, 1932.
Toni, M. S.: Geotechnical and site effect studies in Hurghada City, Red Sea, Egypt, MSc Thesis, Fac. Sci. Assiut. Univ. Assiut, Egypt, 2007.
Ur-Rehman, S., Azeem, T., Abd el-aal, A. K., and Nasir, A.: Parameterization of 18 January 2011 earthquake in Dalbadin Region, Southwest Pakistan, NRIAG J. Astro. Geophys., 2, 203–211, 2013a.
Ur-Rehman, S., Khalid, M., Ali, A., and Abd el-aal, A. K.: Deterministic and probabilistic seismic hazard analysis for Gwadar City, Pakistan, Arab. J. Geosci., 9, 3481–3492, 2013b.
Woo, G.: Kernel estimation methods for seismic hazard area source modeling, B. Seismol. Soc. Am., 86, 353–362, 1996.





NHESSD
3, 7555–7586, 2015

An extended stochastic method for seismic hazard estimation

A. K. Abd el-aal et al.

**Table 1.** The maximum observed and expected magnitudes from identified seismic sources.

| Seismic source | Maximum observed magnitude | Maximum expected magnitude |
|---|---|---|
| 1 | 5.2 | 5.7 |
| 2 | 5.5 | 6 |
| 3 | 4.6 | 4.9 |
| 4 | 6.7 | 6.9 |
| 5 | 4.7 | 4.9 |
| 6 | 5.9 | 6.2 |
| 7 | 4.4 | 4.9 |
| 8 | 4.2 | 4.4 |
| 9 | 4.4 | 4.9 |
| 10 | 5 | 5.4 |
| 11 | 4.2 | 5 |
| 12 | 6 | 6.5 |
| 13 | 4.4 | 4.9 |
| 14 | 6.3 | 6.5 |
| 15 | 4.2 | 4.7 |
| 16 | 6.1 | 6.2 |
| 17 | 5 | 5.4 |
| 18 | 4.7 | 5.1 |
| 19 | 7.2 | 7.3 |
| 20 | 6.3 | 6.4 |
| 21 | 6.9 | 7 |
| 22 | 5.4 | 5.4 |
| 23 | 5.2 | 5.3 |
| 24 | 5.6 | 5.7 |
| 25 | 5.7 | 5.8 |
| 26 | 6.1 | 6.5 |
| 27 | 6.1 | 6.6 |
| 28 | 5.5 | 5.9 |
| 29 | 6.2 | 6.7 |
| 30 | 6.5 | 6.8 |
| 31 | 6.7 | 6.8 |
| 32 | 5.1 | 5.2 |
| 33 | 6 | 6 |
| 34 | 6.9 | 7 |
| 35 | 6.7 | 6.8 |
| 36 | 7.9 | 8 |
| 37 | 7 | 7.1 |
| 38 | 4.1 | 4.6 |
| Back ground | 4.6 | 4.7 |





NHESSD
3, 7555–7586, 2015

**Table 2.** The estimated PGA predicted from the most effective seismogenic sources at the investigated sites in the area of interest.

| City | Effective seismic source | Maximum expected magnitude | PGA ($cm\,s^{-2}$) | |
|---|---|---|---|---|
| | | | Bedrock condition | Surface soil condition |
| Suez | 6 | 6.19 | 44 | – |
| Cairo | 14 | 6.54 | 43.9 | 136.1 |
| Ismailia | 6 | 6.19 | 30.2 | – |
| Zagazig | 14 | 6.54 | 25.3 | 83.3 |
| Port said | 25 | 5.79 | 14.3 | – |
| Damietta | 26 | 6.53 | 14.1 | 48 |





NHESSD
3, 7555–7586, 2015

**Table 3.** The predicted estimated PGA at different frequencies and their corresponding amplification at different locations in the investigated sites in the area of interest.

| City | Frequency | Amplification | | | PGA ($cm\,s^{-2}$) | | |
|---|---|---|---|---|---|---|---|
| | (Hz) | Site 1 | Site 2 | Site 3 | Site 1 | Site 2 | Site 3 |
| Cairo | $F_0$, $A_0$ | 1.5, 4 | 1.5, 3.1 | 1.5, 2.3 | 235.2 | 175.6 | 135.2 |
| | 0.4 | 1 | 1.4 | 1.5 | 58.79 | 79.3 | 88.19 |
| | 0.6 | 0.8 | 0.9 | 1 | 47.03 | 51 | 58.79 |
| | 0.8 | 0.7 | 0.8 | 1.1 | 41.16 | 45.3 | 64.67 |
| | 1 | 0.9 | 0.75 | 1.3 | 52.91 | 42.5 | 76.43 |
| | 2 | 1.9 | 1.45 | 1 | 111.7 | 82.2 | 67 |
| | 4 | 0.6 | 0.8 | 1.7 | 35.28 | 45.3 | 57.95 |
| | 6 | 0.65 | 1.2 | 1.1 | 25 | 42.5 | 57 |
| Damietta | $F_0$, $A_0$ | 1.5, 3.4 | 0.22, 2.7 | 0.25, 1.21 | 47.9 | 40.65 | 16.56 |
| | 0.4 | 1.1 | 1.6 | 1 | 15.5 | 24.09 | 15.06 |
| | 0.6 | 1 | 1.19 | 0.99 | 14.1 | 17.92 | 14.91 |
| | 0.8 | 0.62 | 0.81 | 1.2 | 8.7 | 12.2 | 22 |
| | 1 | 0.8 | 0.9 | 1.12 | 11.3 | 17.55 | 16.86 |
| | 2 | 0.6 | 0.6 | 1.1 | 8.5 | 9.034 | 16.56 |
| | 4 | 0.95 | 0.7 | 1 | 8.2 | 8.5 | 15.06 |
| | 6 | 1.19 | 0.8 | 0.98 | 8.1 | 8 | 14.76 |
| Zagazig | $F_0$, $A_0$ | 0.9, 5.1 | 1.1, 3.3 | 0.7, 1.2 | 286.8 | 88.1 | 64.77 |
| | 0.4 | 3.2 | 0.77 | 0.88 | 180 | 20.6 | 47.49 |
| | 0.6 | 2.8 | 0.59 | 1 | 157.5 | 15.8 | 53.97 |
| | 0.8 | 4 | 1.09 | 1.19 | 225 | 29.1 | 64.23 |
| | 1 | 4.45 | 3.23 | 0.98 | 250.3 | 86.2 | 52.89 |
| | 2 | 1.97 | 2.08 | 1.1 | 110.8 | 55.5 | 59.37 |
| | 4 | 1.82 | 0.61 | 1.11 | 60 | 16.28 | 59.91 |
| | 6 | 0.8 | 0.29 | 1.03 | 44.99 | 11 | 60 |





NHESSD

3, 7555–7586, 2015

**Table 4.** The results of PGA obtained from the uniform hazard spectra on bedrock condition for 75 and 475 years return periods using the probabilistic seismic hazard approach (El-Eraki et al., 2015) at the investigated sites in the study area.

| Period (s) | PGA ($cm\,s^{-2}$) at city | | | | | |
|---|---|---|---|---|---|---|
| | Cairo | | Zagazig | | Damietta | |
| | 75 years | 475 years | 75 years | 475 years | 75 years | 475 years |
| 0 | 38.4 | 120.7 | 35.3 | 115.1 | 31.4 | 64.2 |
| 0.1 | 64.7 | 210.4 | 59.2 | 199.5 | 53.7 | 111.6 |
| 0.2 | 58.7 | 160.4 | 53.8 | 149.4 | 58.3 | 117.8 |
| 0.3 | 48.5 | 118.5 | 44.8 | 108.9 | 51.2 | 101.2 |
| 0.5 | 38.6 | 82.6 | 35.7 | 75.5 | 41.5 | 81.4 |
| 1 | 18.9 | 36.6 | 17.5 | 33.2 | 20.3 | 38.5 |





NHESSD
3, 7555–7586, 2015

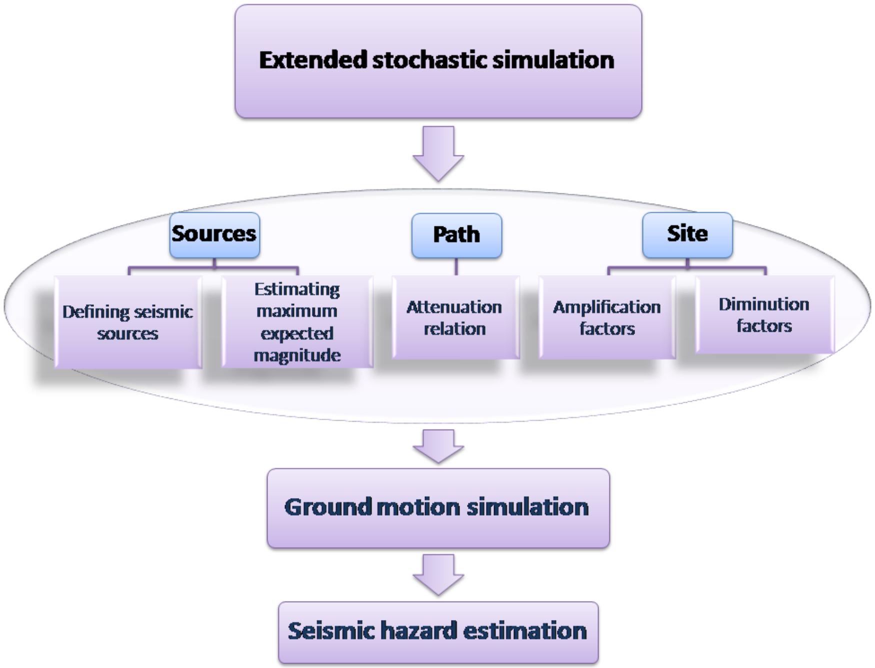


**Figure 1.** The developed extended stochastic simulation for seismic hazard assessment.

NHESSD
3, 7555–7586, 2015

An extended stochastic method for seismic hazard estimation

A. K. Abd el-aal et al.



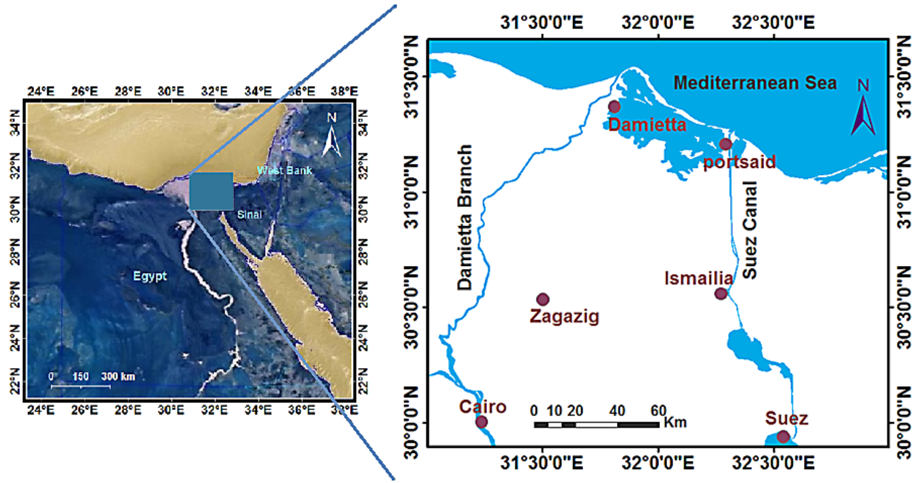


**Figure 2.** Location map of the study area.

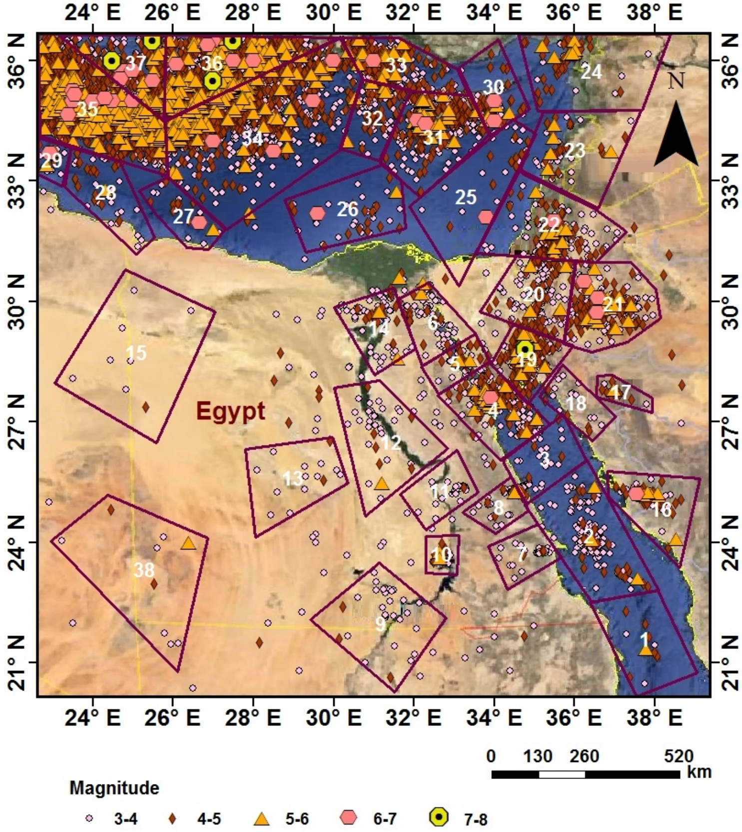


**Figure 3.** Seismicity and seismotectonic source model (updated from the model prepared by El-Eraki et al., 2015).





NHESSD
3, 7555–7586, 2015

An extended stochastic method for seismic hazard estimation

A. K. Abd el-aal et al.

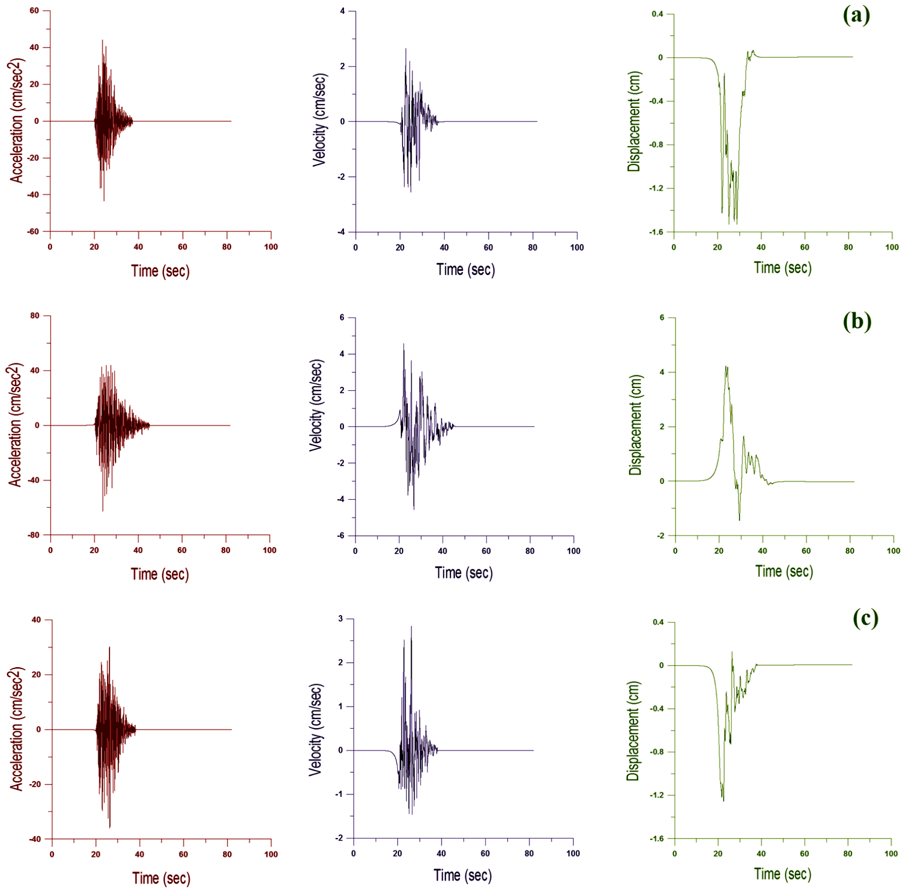


**Figure 4.** The simulated time histories of the expected largest earthquake (acceleration, velocity and displacement) for bedrock condition at: **(a)** Suez, **(b)** Cairo and **(c)** Ismailia cities.





NHESSD
3, 7555–7586, 2015

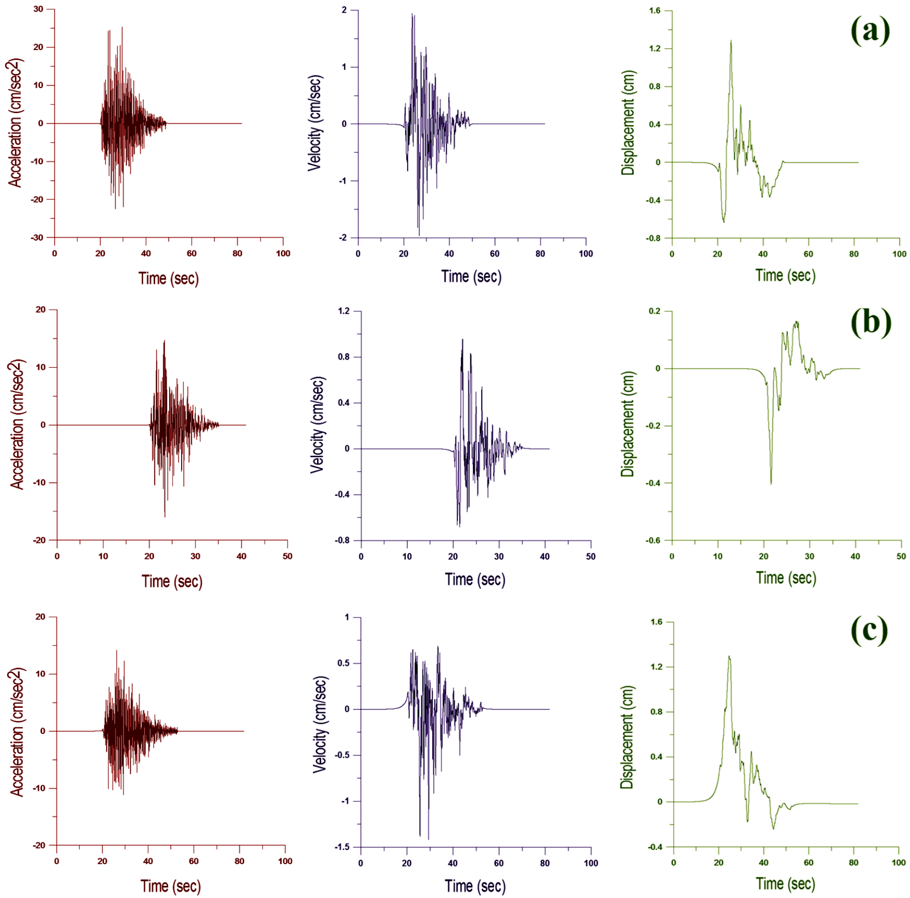


**Figure 5.** The simulated time histories of the expected largest earthquake (acceleration, velocity and displacement) for bedrock condition at: **(a)** Zagazig, **(b)** Port Said and **(c)** Damietta cities.





NHESSD
3, 7555–7586, 2015

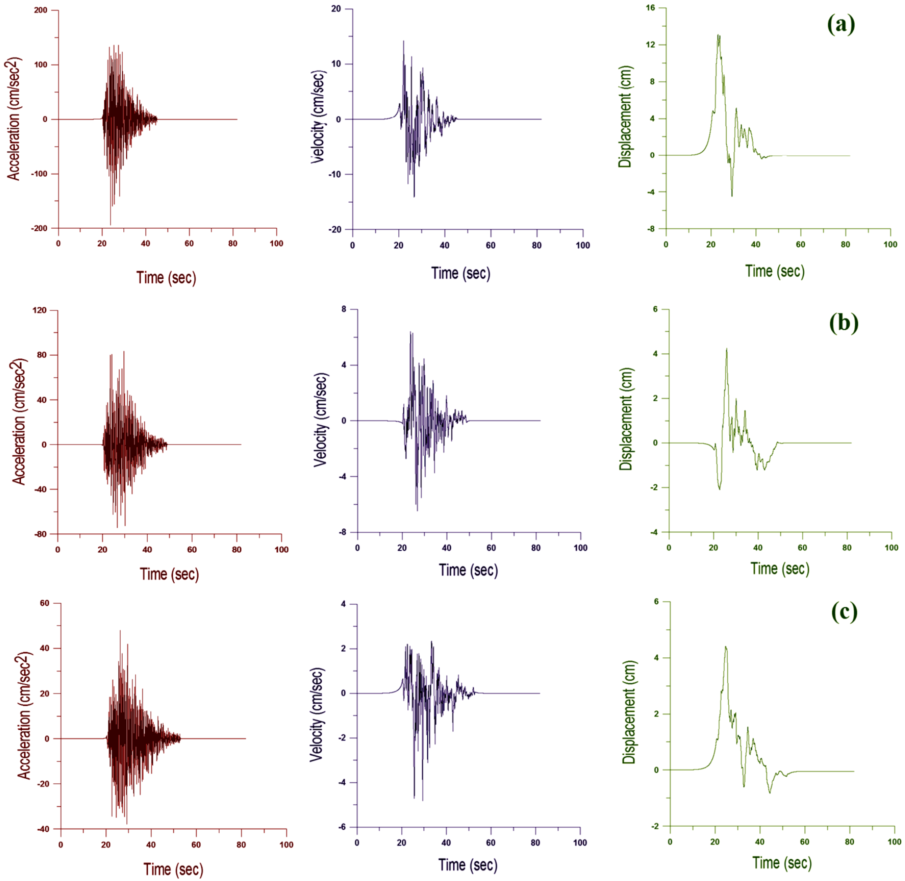


**Figure 6.** The simulated time histories of the expected largest earthquake (acceleration, velocity and displacement) for surface soil condition at: **(a)** Cairo, **(b)** Zagazig and **(c)** Damietta cities.

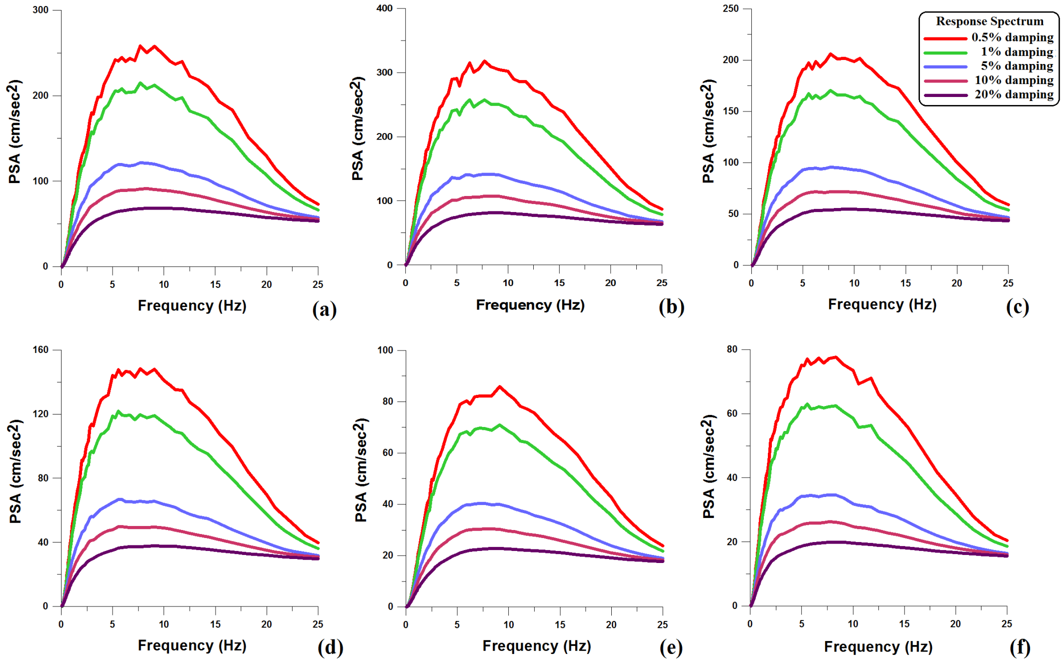


**Figure 7.** The predicted pseudo-spectral accelerations for bedrock condition at: **(a)** Suez, **(b)** Cairo, **(c)** Ismailia, **(d)** Zagazig, **(e)** Port Said and **(f)** Damietta cities.





NHESSD
3, 7555–7586, 2015

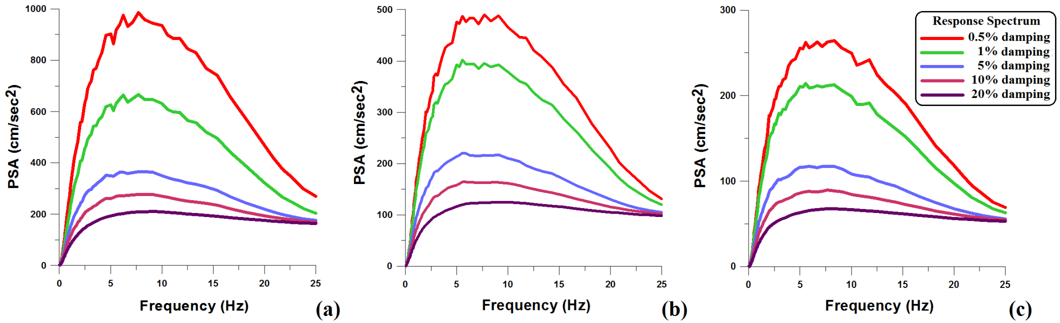


**Figure 8.** The predicted pseudo-spectral accelerations for surface soil condition at: **(a)** Cairo, **(b)** Zagazig and **(c)** Damietta cities.



NHESSD
3, 7555–7586, 2015

NHESSD
3, 7555–7586, 2015

An extended stochastic method for seismic hazard estimation

A. K. Abd el-aal et al.





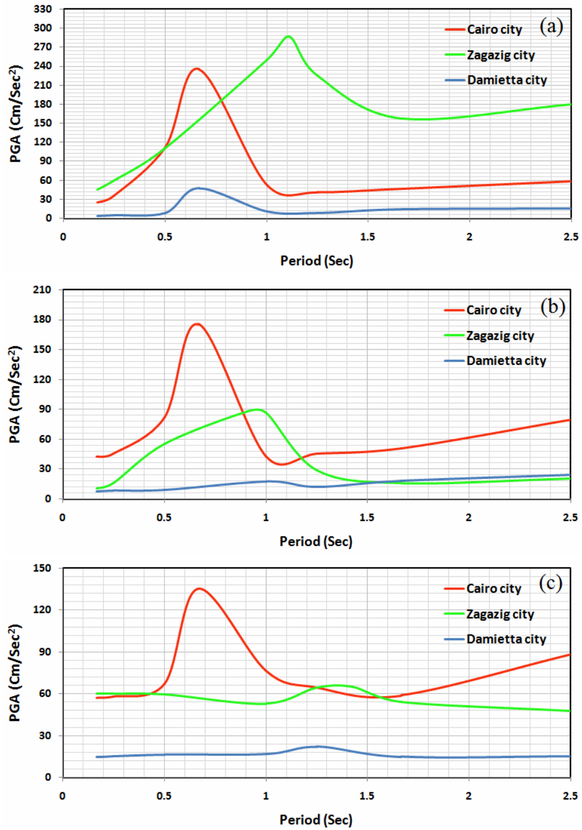


**Figure 9.** The expected PGA obtained from the developed extended stochastic simulation method at each corresponding period (reciprocal of frequency) at the investigated sites. **(a)** Site 1, **(b)** site 2 and **(c)** site 3 at these cities.

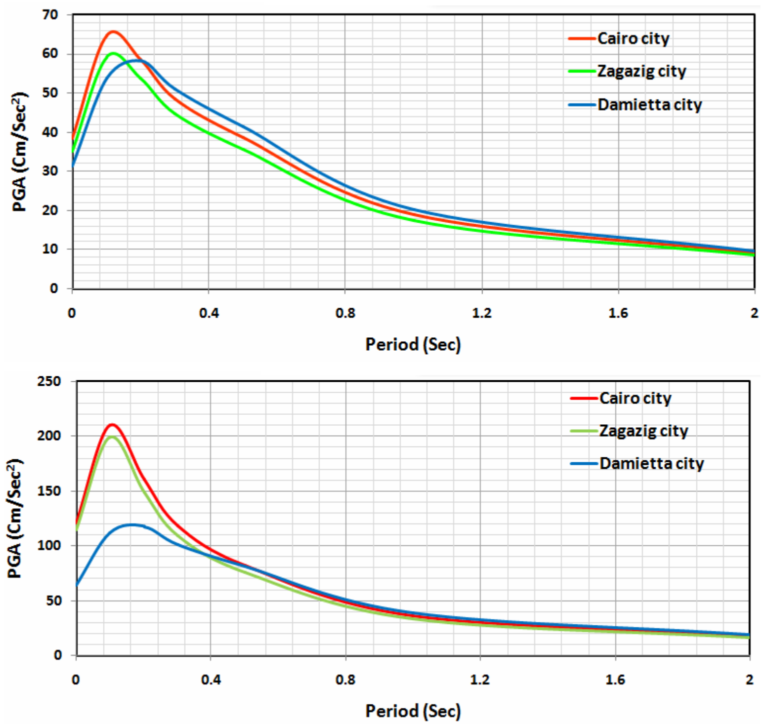


**Figure 10.** The estimated PGA obtained from the uniform hazard spectra on rock sites for **(a)** 75 and **(b)** 475 years return periods using the probabilistic seismic hazard approach (El-Eraki et al., 2015).





NHESSD
3, 7555–7586, 2015

An extended stochastic method for seismic hazard estimation

A. K. Abd el-aal et al.